Biotechnology and Bioprocess Engineering 2009, 14: 738-747
DOI/10.1007/s12257-009-0168-y

Metabolic Profiles of Genetically Modified Potatoes using a Combination of Metabolite Fingerprinting and Multivariate Analysis

Hyun Soon Kim[1†], Suk Weon Kim[2†], Young Seok Park[2], Suk Youn Kwon[1], Jang Ryol Liu[2], Hyouk Joung[1], and Jae Heung Jeon[1*]

[1]Plant system engineering research center, Korea Research Institute of Bioscience and Biotechnology (KRIBB), Daejeon 305-806, Korea
[2]Biological resource center, Korea Research Institute of Bioscience and Biotechnology (KRIBB), Daejeon 305-806, Korea

Abstract Comprehensive metabolite fingerprinting of transgenic potatoes that constitutively express human beta amyloid, curdlan synthase (*CRDS*), and glycogen synthase (*glg*A); and of wild-type potatoes was carried out using FT-IR and ^{1}H NMR spectroscopy in combination with multivariate analyses. Comparison of metabolic patterns between transgenic and wild-type potatoes revealed that there were neither quantitative nor qualitative differences in metabolites between transgenic potatoes expressing human beta amyloid, *CRDS* or *glg*A, and non-transformed control potatoes. However, there were metabolic differences between two control potato lines - one that was fresh and the other stored. After 1 week of storage, comprehensive metabolite patterns were significantly modified. Although the differences between *CRDS* and *glg*A transgenic and control potato lines were small, PCA analysis of FT-IR and ^{1}H NMR spectral data identified two distinct control lines. These results suggest that the comprehensive metabolite changes in control potato lines, which occurred after 1 week of storage, were greater than the differences between *CRDS* and *glg*A transgenic and wild-type potato lines. Thus, the combination of FT-IR and ^{1}H NMR spectral data and multivariate analysis was valuable for the detection of comprehensive differences in metabolic profiles between transgenic and non-transformed control plants, even though peak-signal overlap prevented assignment of pure compounds. The combination of FT-IR and ^{1}H NMR spectral data and multivariate analysis is a simple and rapid method for evaluation of the metabolic equivalence of GM crops. © KSBB

Keywords: FT-IR spectroscopy, genetically modified potatoes, ^{1}H NMR spectroscopy, multivariate analysis, principal component analysis (PCA)

INTRODUCTION

The potato is one of four major crops that are of great agronomic interest. In addition, the potato is a model plant for the evaluation of chemical, physical and environmental effects, and for use in genetic studies. Application of genetic engineering technology to plants resulted in the production of many transgenic potato lines during the past decade. When transgenic plants express a foreign, *i.e.* non-potato, gene, the composition of the transgenic potato tuber must be evaluated to ensure its safety for human consumption, regardless of whether the foreign gene is related to a metabolic pathway. Another concern regarding transgenic plants is the introduction of unforeseen traits into crops during genetic engineering, resulting in undesirable metabolites [1].

A fundamental issue in assessment of the safety of genetically modified crops is identification of unintentional changes in genetically modified crops. One approach to address this concern is the use of metabolomics [2]. Metabolomics is emerging as an important research tool along with the other "-omics" fields, such as transcriptomics and proteomics. Metabolomics aims to identify and fully characterize low-molecular-weight metabolites in living cells, tissues, and whole organisms [3]. Metabolite fingerprinting, a branch of metabolomics, identifies clusters of similar compounds that are used to classify individual samples. Therefore, metabolite fingerprinting usually involves de-

† Both the authors contributed equally to this work.
***Corresponding author**
Tel: +82-42-860-4492 Fax: +82-42-860-4677
e-mail: jeonjh@kribb.re.kr

termination of spectra crude solvent extracts, rather than purification and isolation of individual compounds under standardized conditions. Moreover, the technique ignores individual peak assignments in the complex NMR and IR spectra. To extract useful biological information from the complex spectral data set, metabolite fingerprinting techniques are combined with multivariate statistical methods, such as principal component analysis (PCA) and discriminant function analysis (DA). The metabolites responsible for the classification of individual samples can be identified from the score loadings generated by PCA and related techniques [4]. Thus, metabolic profiles are revealed in the information obtained for the various metabolites in the sample. Metabolite fingerprinting may have wide application in the fields of metabolic engineering and molecular breeding. To date, metabolomics has been used successfully in numerous plant species, including *Arabidopsis* [5-7], strawberry [8], potato [9,10], *Medicago* [11], *Populus* [12], tomato [13], and rice [14]. Therefore, metabolite fingerprinting provides a rapid method for the initial, less-selective screening of overall compositional changes in genetically modified crops. In addition, recent research efforts have sought to fully describe the compositional profiles of metabolites present in conventional crop varieties and to compare them with corresponding profiles of genetically modified crops, including potatoes [2,15], tomatoes [16], rice [17], and wheat [18,19].

Transgenic plants that express foreign genes must be thoroughly examined prior to commercial application. First, transgenic plants may have distinct characteristics due to introduction of foreign genes. Moreover, transgenics may have undesirable characteristics due to knockout of specific genes concurrent with introduction of foreign genes. There are several biological assays and analytic techniques that could readily detect these transgene effects. However, determination of the specific functional consequences of gene knockout in transgenic plants is very difficult, even though the insertion loci are fully identified. To address these issues, we examined the possibility that similarities in comprehensive metabolite fingerprinting patterns of whole-cell extracts may reflect both knockout and transgene metabolic effects in transgenic plants. First, transgenic plants expressing a foreign gene that is not related to plant metabolic pathways were prepared. Introduction of human-derived 5Aβ42 resulted in constitutive expression of beta amyloid (Aβ) in the potato plants [20,21]. Second, transgenic plants expressing foreign genes that are involved in metabolic pathways, *i.e.* curdlan synthase (*CRDS*) and glycogen synthase (*glg*A) [22] were prepared. To examine the possibility that metabolite fingerprinting patterns could be used to evaluate the substantial equivalence of genetically modified potatoes, we examined the effects of 1 week of storage in control potatoes. Using two different kinds of transgenic and control potato lines, we examined the possibility that FT-IR (Fourier transform infrared) and ^{1}H NMR spectroscopy, in combination with multivariate analysis, may allow for metabolic discrimination between transgenic and wild-type potatoes.

MATERIALS AND METHODS

Plant Material, Growth Conditions, and Genetic Transformation

The commercial potato (*Solanum tuberosum* L.) cultivars, Désirée, was vegetatively propagated from cuttings using an MS medium [23] containing 3% (w/v) of sucrose at 24ºC in a growth chamber (24ºC day/24ºC night, 80 μmol/m^2/s^1 from cool-white fluorescent lamps with a 16 h photoperiod). Transgenic lines were obtained by leaf disc transformation, according to Stiller *et al.* [24] using an *Agrobacterium tumefaciens* strain, LBA4404 containing pE5AβS, which is a human beta amyloid expression vector [20]. Briefly, leaf discs from 2-week-old *in vitro* cultures of *S. tuberosum* were co-cultivated with *A. tumefaciens*. After 2 days of co-cultivation, the leaf discs were placed on an MS medium containing 3%, sucrose (w/v); 0.01 mg/L, naphthalene acetic acid; 0.1 mg/L, gibberellic acid; 2 mg/L, trans-zeatin riboside; 500 mg/L, carbenicillin; 100 mg/L, kanamycin; and 0.8%, agar. Regenerated shoots were excised and placed in MS medium containing carbenicillin for rooting. Three-week-old tissue culture-originated control plants and their transgenic derivatives were transferred to pots and cultivated under greenhouse conditions. The sprouting behavior of tubers harvested from 4-month-old plants, which had been grown in the greenhouse, was examined after 90 days of storage at room temperature. The tubers were planted in pots and watered regularly.

CRDS-expressing potato lines under control of CaMV35S or granule-bound starch synthase (GBSS) promoters and *glg*A-expressing potato lines controlled by the CaMV35S promoter were obtained by leaf disc transformation using the *A. tumefaciens* strain, LBA4404, harboring the *CRDS* and *glg*A genes [22], respectively. Transgenic *CRDS*- and *glg*A-expressing potato lines were cultivated and collected as described above. The plants that were used in the experiments are described in detail in the Table 1.

Production of Tubers for Analysis

Plants were grown from tubers in 30 cm diameter pots. Three seed tubers were planted for each transgenic or control line. Plants were organized in a random block design within the growing facility. After natural senescence, tubers were harvested and analyzed. Tuber number, fresh weight yield (per plant), and dry matter content were determined. Thereafter, three tuber samples ('Sets') from each plant (Rep) were set aside, resulting in 3 sets of samples per replicate plant. In some cases, each of the three sets comprised a single tuber. In other cases, it was necessary to combine smaller tubers to provide a replicate sample of the desired fresh weight (ca.100 g FWT).

Effect of Cold Storage on the Metabolic Change of Potato Tubers

After natural senescence, tubers (*S. tuberosum* L. cv. Désirée) were harvested and analyzed. To determine the effects of

Table 1. Plant materials used in the preparation of whole-cell extracts of potato tubers

Sample label	Cultivar	Transgene	Storage	Color of tuber crossection
Control 1	Desiree	Wild	No	White
Control 2	Desiree	Wild	Storage for 1 week	Pale yellow
T2	Desiree	β-amyloid	No	White
T8	Desiree	β-amyloid	No	White
CRDS-1	Desiree	*crds*	No	White
CRDS-5	Desiree	*crds*	No	Pale yellow
CRDS-11	Desiree	*crds*	No	Pale yellow
glgA-1	Desiree	*glg*A	No	White
glgA-4	Desiree	*glg*A	No	White

storage on metabolite profile, tubers were harvested and immediately stored at −70ºC. Other tubers were stored for 1 week at 4ºC. After cold storage, tubers were transferred and stored at −70ºC before use. To minimize the effect of tuber growth-stage on metabolic change, tubers of similar size were selected and used in preparation of whole-cell extracts.

Whole-cell Extract Preparation and FT-IR Spectroscopy

Whole-cell extracts were prepared for FT-IR spectroscopy and spectral data processing using a method previously reported for strawberries [25]. The inner flesh of each potato was collected, freeze-dried, ground to a fine powder, and stored at −70ºC. Fifty milligrams of the powdered sample and 1 mL of 20% (v/v) methanol were mixed in an Eppendorf tube (1.5 mL). Then, the solution was incubated for 10 min in a 50ºC water bath and centrifuged for 5 min at 12,000 rpm. Five microliters of supernatant was dropped onto a silicon plate and allowed to dry for 15 min at 30ºC. Samples of homogenized whole-cell extract from each tuber were run in triplicate.

FT-IR spectra were measured using a Bruker Tensor 27 FT-IR spectrometer equipped with an HTS-XT high-throughput and automated collection system. A globar source and DTGS detector were used. Three spectra were acquired for each sample and each IR spectrum corresponded to the accumulation of 128 scans. Infrared spectra were obtained by subtraction of the spectra (background), onto which the samples were deposited. Spectral resolution was 4 cm^{-1} and spectra were collected over wave numbers ranging from 4,000 to 400 cm^{-1}. Spectra were processed using the OPUSLab program (ver. 5.5, Bruker Optics Inc.). FT-IR spectra were collected during three separate analyses.

^{1}H NMR Spectroscopy of Whole-cell Tuber Extracts

Fifty-milligram samples of freeze-dried powder were weighed and placed into sterile 1.5 mL Eppendorf tubes. One milliliter of deuterated solvent mixture (v/v, D_2O: CD_3OD, 80:20) containing 0.005% (w/v) sodium salt of trimethylsilylpropionic acid (TSP-d_4) was added to each sample. The contents of the tube were mixed thoroughly and heated in a 50ºC water bath for 10 min. After cooling, the samples were centrifuged at 12,000 rpm for 5 min. Seven hundred and fifty microliters of supernatant was transferred to a 5 mm NMR tube. All ^{1}H NMR spectra were obtained with a Varian Unity 500 NMR spectrometer equipped with a linear amplifier in the observe transmitter channel. The HOD peak at 4.76 ppm was pre-saturated to eliminate spectral overlapping. Each spectrum was acquired by accumulation of 32 scan repetitions. The ^{1}H NMR chemical shifts in the spectra were referenced to TSP-d_4 at 0.00 ppm. Samples of homogenized whole-cell extracts from each treatment were run in triplicate.

Spectral Data Processing and Multivariate Analysis of FT-IR and ^{1}H NMR Spectra

For FT-IR spectral data processing, spectral data were first subjected to baseline correction and pre-processing by second derivation using R software (ver. 2.5). Noise caused by equipment error was reduced by subtraction, thereby calculating spectral data with equivalent intervals. Spectral data were collected and saved as ASCII-compatible files. The pre-processed spectral data from each sample were analyzed using PCA (principal component analysis). After PCA analysis, all samples were located in the PCA-score plot and the Euclidian distance between samples was then calculated. Hierarchical clustering analysis and Fisher's linear discriminant function analysis (LDA) were performed using this procedure. Hierarchical dendrograms were constructed from PCA of the FT-IR data using the non weighted pair group method and an arithmetic mean analysis (UPGMA) method with the Euclidean distance as the indicator of similarity. PCA scores extracted from the PCA analysis were used in DA (discriminant analysis) and HCA (hierarchical clustering analysis) to classify potato tubers.

For ^{1}H NMR spectral data processing, the ^{1}H NMR spectra were automatically converted to ASCII files with an automatic baseline correction using an ACD/NMR Processor (ver. 7.0, Advanced Chemistry Development, Canada). Spectral intensities were scaled to TSP-d_4, and were adjusted to equal width, corresponding to the region between 10.5 and −0.5 ppm. In addition, peak alignment procedures for ^{1}H NMR spectra were performed using SpecAlign (ver. 2.3) software [26]. At this stage, the residual proton signal corresponding to TSP–d_4 (δ 0.0) was removed. The resulting ASCII file was imported into R software (ver. 2.5) and several multivariate analyses were performed, as described for the FT-IR spectral data.

RESULTS AND DISCUSSION

Tuber Yield and Sprouting Behavior of Aβ-overexpressing Potato Lines

To examine phenotypic variation, tuber yield and sprout-

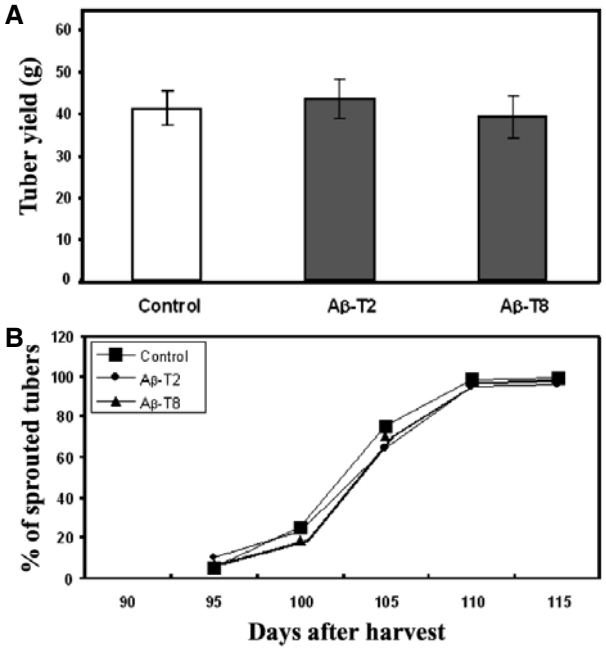

Fig. 1. (A) Tuber yield and (B) sprouting behavior of human beta amyloid-producing potatoes and non-transformed control potato. Tuber yields were measured in 10 pots per line and are reported as the average yield per pot ± SD. Sprouting behavior was evaluated in tubers stored for 90 days at room temperature. Ten tubers from each line were planted in pots in the greenhouse and the number of emergent stems was determined.

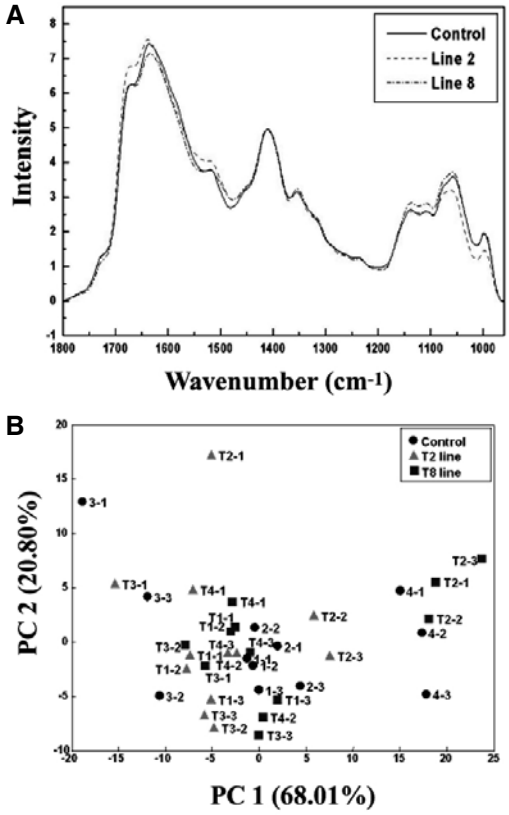

Fig. 2. Representative (A) FT-IR spectra and (B) PCA-score plots of human beta amyloid-producing potatoes and non-transformed control potatoes. (A) Averaged spectra for replicates of the control line (——), the beta amyloid-producing T2 line (•••••), and the beta amyloid-producing T8 line (—•—). (B) Two-dimensional PCA-score plot of FT-IR data for human beta amyloid-producing potatoes and non-transformed control potato. The first two principal components, which account for 68.01 and 20.80% (88.81% total) of the total variation, respectively, are shown. (●), Control; (▲), the beta amyloid-producing T2 line; and (■), the beta amyloid-producing T8 line. Numbers represent four individual plants from each potato line and three replicates of the FT-IR spectra for each plant.

ing behavior of two Aβ-overexpressing lines and control lines were determined (Fig. 1). Total tuber yield from 4-month-old control plants was 41.5 ± 10 g of fresh weight. Whereas Aβ-overexpressing potatoes showed yields of 43.5 ± 10 (line T2) and 38.5 ± 10 (line T8), as shown in Fig. 1A. There was no statistically significant difference in tuber yield between the two Aβ-overexpressing lines and the control lines. These results indicate that overexpression of Aβ does not affect tuber yield. We also examined the sprouting behavior of tubers after storage for 90 days at room temperature. There was no difference in sprouting behavior between the Aβ-overexpressing and control lines (Fig. 1B). These results indicate that overexpression of Aβ does not influence tuber sprouting behavior after a period of storage. Thus, we concluded that overexpression of Aβ in potato tubers does not affect the major agronomic characteristics of potato, including tuber yield and sprouting behavior.

Metabolic Evaluation of Aβ-overexpressing Potato Lines by FT-IR and ^{1}H NMR Spectral Analysis

Representative FT-IR spectra of two Aβ-overexpressing lines and a control line are shown in Fig. 2. Based on the FT-IR spectra, there were no significant differences in the metabolite profiles between Aβ-overexpressing and control lines (Fig. 2A). This result indicates that overexpression of Aβ affects neither the quantity nor the quality of metabolites relative to wild-type potatoes. FT-IR metabolite fingerprinting data were analyzed using PCA (Fig. 2B). The first two principal components are displayed, accounting for 68.01 and 20.80% (88.81% total) of the total variation, respectively. Replicate samples of each line were distributed in discrete clusters, indicating that PCA was able to discriminate among lines. However, the first principal component (PC)-score axis of the scores plot showed no separation into transgenic and control Désirée lines, although the first principal component (PC) accounted for greater than 68.01% of the total

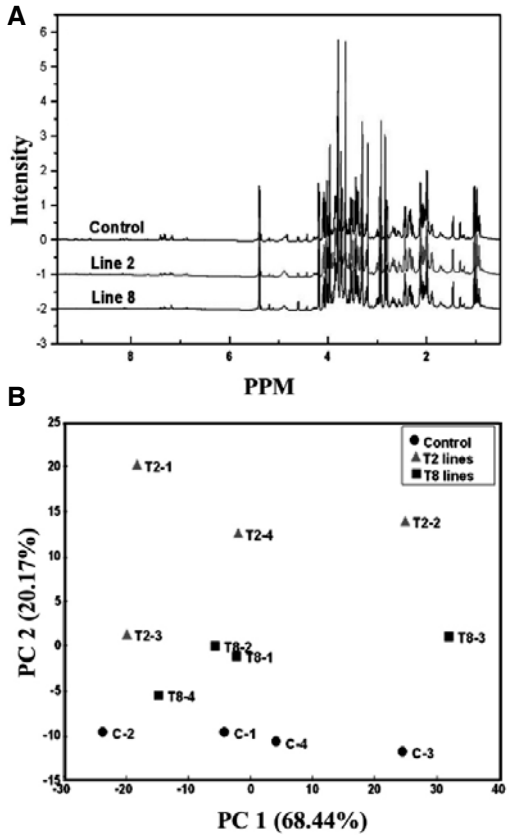

Fig. 3. Representative (A) ^{1}H NMR spectra and (B) PCA-score plot of human beta amyloid-producing potatoes and non-transformed control potato. (A) Averaged replicate spectrafor control (—), the beta amyloid-producing T2 line (—), and the beta amyloid-producing T8 line (—). (B) Two-dimensional PCA-score plot of ^{1}H NMR spectral data of human beta amyloid-producing potatoes and non-transformed control potato. The first two principal components, which account for 68.44 and 20.17% (88.61% total) of the total variation, respectively, are shown. (●), Control; (▲), beta amyloid-producing T2 line; and (■), beta amyloid-producing T8 line. Numbers represent four individual plants from each potato line.

variation. Similarly, the PC 2-score axis did not discriminate between transgenic and control lines. Using *t*-tests, comparison of mean PCA scores between the two Aβ-overexpressing lines and a control line confirmed a single population. These results indicate that the inter-plant metabolic variance within each line was far greater than the variance among lines. Thus, we concluded that the metabolic pattern does not discriminate between the two Aβ-overexpressing lines and the control lines, even though Aβ-overexpression was confirmed by molecular biological analysis [20].

Representative ^{1}H NMR spectra of two Aβ-over expressing lines and a NT line are shown in Fig. 3. Similar to the FT-IR results, ^{1}H NMR spectra also indicated no significant differences in metabolic pattern between Aβ-overexpressing and control lines (Fig. 3A). PCA scores obtained from the ^{1}H NMR data were plotted in two dimensions using the first two principal components, which accounted for 68.44 and 20.17% (88.61% total) of the total variation, respectively, as shown in Fig. 3B. Although the first two PC explained greater than 88.6% of the total variation, the first PC-score axis did not show any separation of the lines into sub-groups. These results are identical to those obtained using FT-IR (Fig. 2). However, the PC 2-score axis of the ^{1}H NMR score plot shows a greater degree of discrimination between the Aβ-overexpressing line, T2, and the control line (Fig. 3B). Comparison of mean PCA-score-plot values for the Aβ-overexpressing T8 line and the control line by *t*-test confirmed a single population. However, the Aβ-overexpressing T2 line and the control line were significantly different based on comparison of the mean scores using a *t*-test. These results indicate that there are no major metabolic differences between the two Aβ-overexpressing lines and the control line, although there was a small difference in metabolic pattern between the Aβ-overexpressing T2 line and the control line. This observation raises the possibility that variation in metabolic pattern within a particular transgenic line may result from both transgene and gene-knockout effects. Based on the results of the present study, we concluded that the comprehensive metabolic pattern of the Aβ-overexpressing T8 line was more similar to that of the control plant than to that of the T2 line. In this study, we did not examine all potato metabolites, nor did we elucidate loci. However, we inferred that the Aβ-overexpressing T8 line did not exhibit an undesirable gene-knockout effect compared with the Aβ-overexpressing T2 line based on comprehensive metabolite fingerprinting of whole-cell extracts.

Recently, comparison of complete compositional profiles between conventional crop varieties and corresponding genetically modified crops, including potatoes [2,15], tomatoes [16], rice [17], and wheat [18,19] has been the focus of intensive research efforts. Catchpole *et al.* [2] reported that multivariate analysis of GC-ToF-MS data allowed for discrimination between transgenics and Désirée controls. They also showed that metabolic discrimination was significantly diminished by removal of metabolite peaks that were directly related to the transgene. In the present study, we found that Aβ-overexpressing transgenic potatoes did not show discrete unique metabolic discrimination patterns that differed from control plants. Therefore, based on simplicity, convenience, and reproducibility of the method, we concluded that the combination of FT-IR, ^{1}H NMR, and multivariate analysis could be used to evaluate metabolic differences between transgenic and control plants.

Evaluation of Metabolic Changes that Occur During Cold Storage of Potatoes Using FT-IR and ^{1}H NMR Spectral Analyses

To evaluate differences in metabolic patterns between fresh Désirée tubers and those that had been stored for 1 week, we conducted PCA analysis of FT-IR and ^{1}H NMR spectral data. Average FT-IR (Fig. 4A) and ^{1}H NMR (Fig.

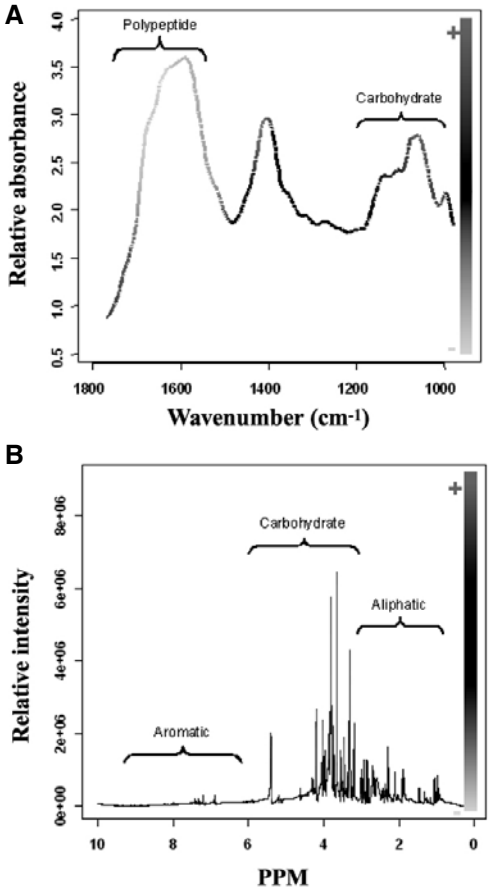

Fig. 4. Representative (A) FT-IR and (B) ^{1}H NMR spectra from fresh (control 1) and stored (1 week) Desiree tubers (control 2). A significant difference between the spectra of Desiree control 1 and control 2 was shown by *t*-test. The red portion of the spectrum represents the FT-IR spectral region, in which stored tubers (control 2) showed a significant increase in spectral absorbance compared with fresh tubers (control 1). In contrast, the green portion of the spectrum represents the FT-IR spectral region, in which stored tubers showed a significant decrease in spectral absorbance compared with fresh tubers. Color intensity is proportional to the *p*-value.

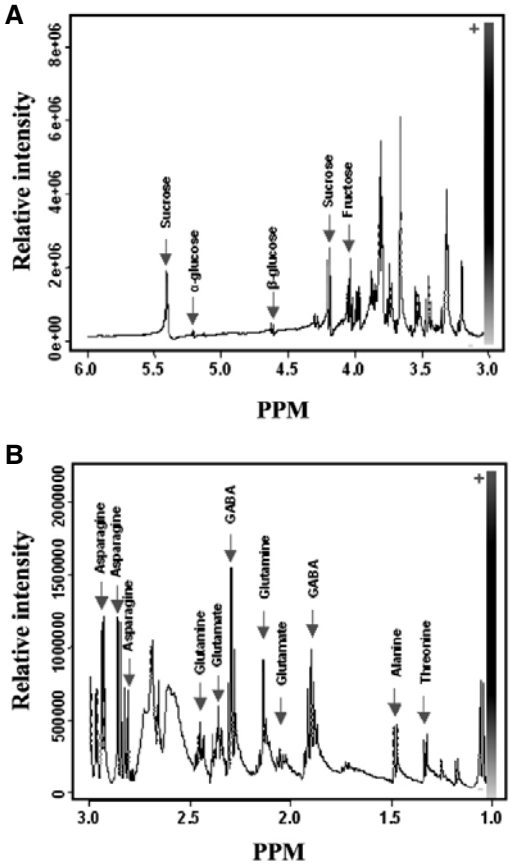

Fig. 5. Peak assignments in ^{1}H NMR spectra for (A) carbohydrate, and (B) aliphatic regions of fresh (control 1) and stored (control 2) Desiree tubers.

4B) spectra from fresh (control 1) tubers and those that had been stored for 1 week (control 2) are shown in Fig. 4. The FT-IR spectral pattern was markedly changed after storage. FT-IR spectroscopy showed that there was a significant increase (greater than two-fold) in spectral absorbance in the region between 1,000~1,200 cm^{-1}, whereas the absorbance decreased significantly in the regions between 1,400~1,450 cm^{-1} and 1,500~1,750 cm^{-1} (Fig. 4A). Although we could not assign these FT-IR spectral regions to pure compounds, carbohydrates, polypeptides, and amino acids were responsible for specific peak signals in these FT-IR regions. Based on changes in these peak signals, we concluded that one week of storage caused a significant increase in carbohydrates and a decrease in amino acids. The FT-IR results were confirmed by ^{1}H NMR metabolite fingerprinting. In the ^{1}H NMR, overlapping peak signals in the carbohydrate region of the spectrum were dramatically increased in tubers that had been stored for one week, whereas peak signals in the aliphatic region of the ^{1}H NMR spectrum were decreased in the stored tubers (Fig. 4B). Peak signals in the carbohydrate (Fig. 5A) and aliphatic (Fig. 5B) regions of the ^{1}H NMR spectrum were assigned based on the chemical shift of a pure compound, ^{1}H NMR DB (SDBS web site). Peak signals from soluble sugars including sucrose, glucose, and fructose, increased after storage whereas aliphatic and aromatic amino acids, including threonine, alanine, GABA, glutamine, and asparagines, decreased. Based on these results, we concluded that storage of tubers for 1 week significantly altered sugar and amino acid composition.

The PCA score (Fig. 6A) and loading plots (Fig. 6B) obtained from the FT-IR spectral of the fresh and stored tubers were used to evaluate the effects of tuber storage. The first two principal components, which accounted for 85.89 and 10.56% (96.45% total) of the total variation, respectively, are shown in Fig. 6A. The first PC axis of the score plot distinguished between two groups, which corresponded to the

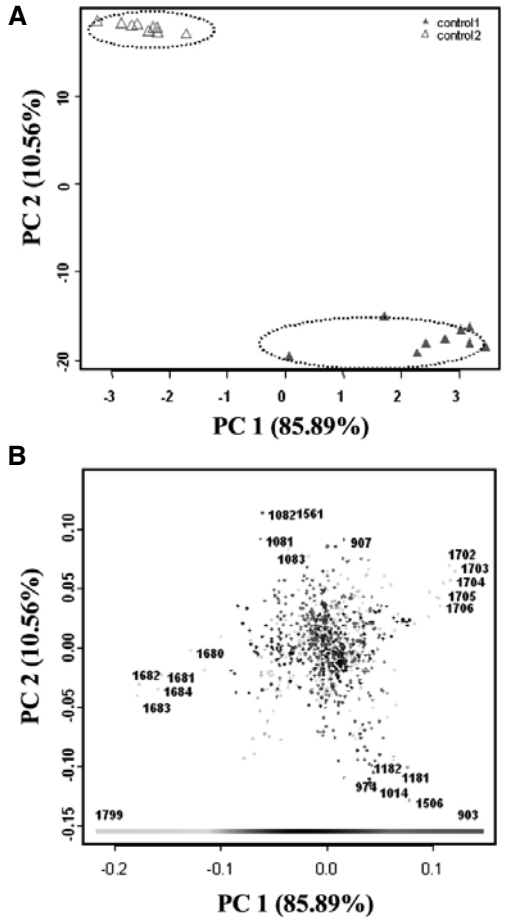

Fig. 6. (A) PCA-score plot, and (B) loading plot from FT-IR spectral data from fresh (control 1) and stored (control 2) Desiree tubers. (A) Two-dimensional PCA score plot of FT-IR data from fresh (control 1) and stored (control 2) Desiree tubers. The first two principal components, which accounted for 85.89 and 10.56% (96.45% total) of the total variation, respectively, are shown. (B) PCA-score loading plot of FT-IR data from fresh and stored Desiree tubers. Symbols represent replicates of each tuber line. Numbers represent variables that are important for discrimination between fresh and stored tubers.

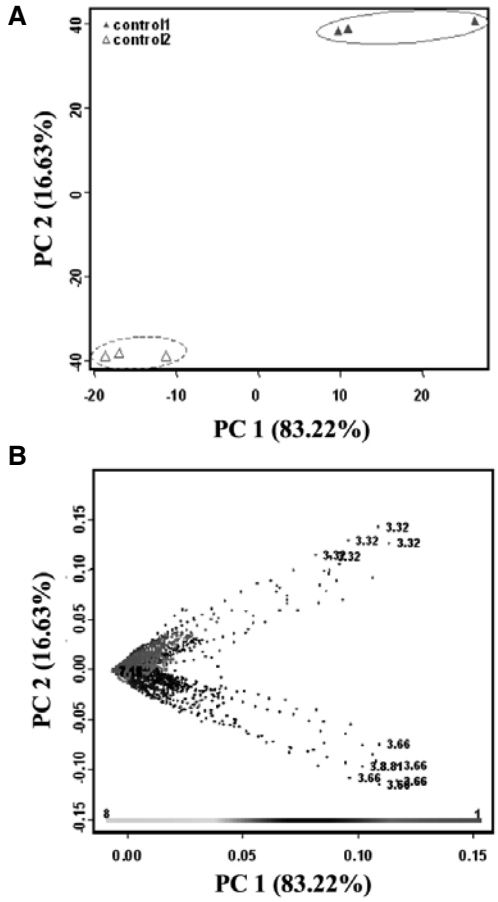

Fig. 7. (A) PCA-score plot and (B) loading plot for ^{1}H NMR spectral data from Desiree tubers. (A) Two-dimensional PCA-score plot of FT-IR data from fresh (control 1) and stored (control 2) Desiree tubers. The first two principal components, which accounted for 83.22 and 16.63% (99.85% total) of the total variation, respectively, are shown. (B) PCA-score loading plot of FT-IR data from fresh and stored Desiree tubers. Symbols represent replicates of each tuber line. Numbers in (B) represent variables that are important for discrimination between fresh and stored tubers.

stored and fresh tubers (Fig. 6A). The PC loading plot indicated that the regions of the FT-IR spectra between 900~1,080 cm^{-1} and 1680~1710 cm^{-1} were responsible for the group separation (Fig. 6B). We also examined the PCA score (Fig. 7A) and loading (Fig. 7B) plots from the ^{1}H NMR spectral data. The first two principal components, which accounted for 83.22 and 16.63% (99.85% total) of the total variation, respectively, are shown in Fig. 7. The first PC axis of the score plot showed separation into two groups, which corresponded to the stored and fresh tubers (Fig. 7A). The PC loading plot indicated that the 3.32, 3.66, and 3.81 ppm regions of the ^{1}H NMR spectra were responsible for the group separation (Fig. 7B). Results of both PCA and loading analyses of FT-IR (Fig. 6) and ^{1}H NMR (Fig. 7) spectra showed that discrimination between fresh and stored tubers was possible. The most important variables for group separation were derived from soluble sugars and aliphatic amino acids, as shown in the quantitative FT-IR and ^{1}H NMR spectra (Figs. 4 and 5).

Metabolic Evaluation of *CRDS*- and *glg*A-overexpressing Potato Lines by FT-IR and ^{1}H NMR Spectral Analyses

To evaluate differences in metabolic patterns among several *CRDS*- and *glg*A-expressing potato tubers and two control lines of Désirée tubers, we conducted PCA, LDA, and

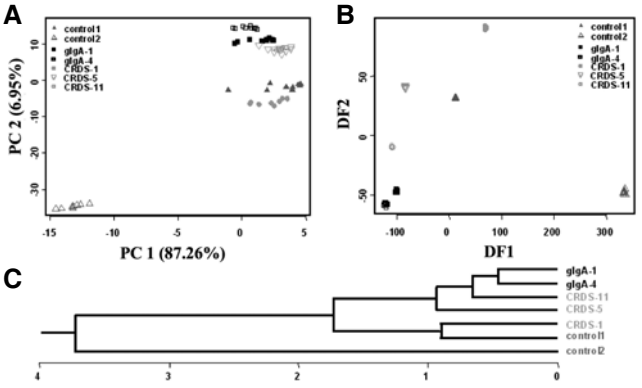

Fig. 8. (A) PCA-score plot, (B) LDA-score plot, and (C) dendrogram of HCA for FT-IR spectral data from several *CRDS*- or *glg*A-expressing potato tubers and two control Desiree tubers (control 1 and 2). (A) Two-dimensional PCA-score plot of FT-IR data. The first two principal components, which accounted for 87.26 and 6.95% (94.21% total) of the total variation, respectively, are shown. (B) LDA-score plot of PCA-score data. (C) Dendrogram based on HCA of the PCA-score data. Symbols represent replicates of each tuber line.

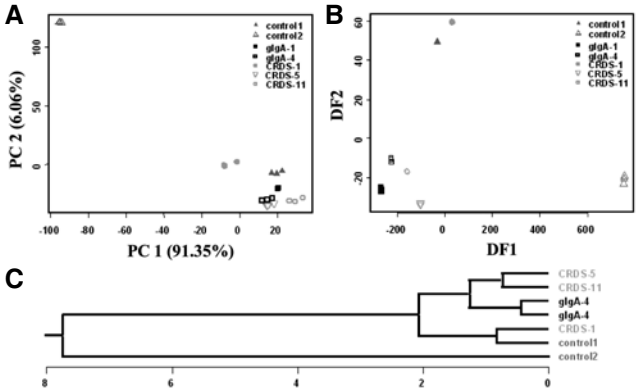

Fig. 9. (A) PCA-score plot, (B) LDA-score plot, and (C) dendrogram of HCA for ^{1}H NMR spectral data from several *CRDS*- or *glg*A-expressing potato tubers and two control Desiree tubers (Control 1 and 2). (A) Two-dimensional PCA-score plot of FT-IR data. The first two principal components, which accounted for 91.35 and 6.06% (97.41% total) of the total variation, respectively, are shown. (B) LDA-score plot of PCA-score data. (C) Dendrogram based on HCA of the PCA-score data. Symbols represent replicates of each tuber line.

HCA analyses of the FT-IR (Fig. 8) and ^{1}H NMR (Fig. 9) spectral data. The first two principal components, which account for 87.26 and 6.95% (94.21% total) of the total variation, respectively, are shown in Fig. 8A. Interestingly, when several *CRDS*- and *glg*A-expressing potato tuber lines were included in the PCA analysis, the first PC axis of the score plot showed separation into two distinct groups: the tubers that were stored for one week; the *CRDS*- and *glg*A-expressing potato tuber lines and fresh Désirée tuber controls (Fig. 8A). These separation patterns are identical to the pattern observed for the fresh and stored Désirée tubers shown in Fig. 6A. The second group could be further separated into two sub-groups. The first sub-group consisted of the fresh control and *CRDS*-1 lines. The second sub-group consisted of the *CRDS*-11, *CRDS*-5, *glg*A-1, and *glg*A-4 lines. These separation patterns were confirmed by DA (Fig. 8B) and HCA (Fig. 8C) analyses.

For the ^{1}H NMR (Fig. 9) spectral data, the first two principal components, which accounted for 91.35 and 6.06% (97.41% total) of the total variation, respectively, are shown in Fig. 9A. The separation pattern of the major group by PCA (Fig. 9A), DA (Fig. 9B), and HCA (Fig. 9C) analyses of the ^{1}H NMR spectral data was identical to the results of the FT-IR analyses (Fig. 8), although there were subtle differences in the sub-group branching patterns. These results suggest that there is a distinct metabolic difference between fresh tubers and those that have been stored for 1 week, whereas metabolic differences between *CRDS*- or glgA-expressing transgenic and control lines were not large enough to result in a discrete clustering pattern. HCA analysis was used to compare FT-IR and ^{1}H NMR spectra of fresh control and *CRDS*-1-expressing lines, which were members of the first sub-group (Fig. 8C). No significant differences in FT-IR (Fig. 10A) and ^{1}H NMR (Fig. 10B) spectra were observed between the fresh control and *CRDS*-1 lines. Baker *et al.* [18] reported similar results in a metabolomic study of genetically modified wheat. These investigators concluded that differences between control and transgenic lines are generally of the same magnitude as differences between control lines grown on different sites or during different years. Similarly, in the present study, results of FT-IR and ^{1}H NMR spectral analyses clearly demonstrate that transgenic lines expressing foreign genes, independent of their role in plant metabolic pathways, are substantially equivalent to wild-type potatoes (Figs. 2, 3, and 10).

Unintended changes in crops are known to result from traditional breeding [27] and somaclonal variation [28]. If the PCA scores of many transgenic lines are analyzed by plotting the scores, transgenic lines with metabolic similarities will form clusters in the PCA-score plot. In transgenic plants, the transgene and knockout (position) effects are the most important determinants of metabolic similarity. Therefore, the balance between the strength of the transgene and knockout effects will determine the clustering pattern on the PCA score plot. Thus, we propose that the combination of FT-IR and ^{1}H NMR spectral data and multivariate analysis be applied as an efficient and rapid analytical tool for metabolic discrimination between transgenic and control lines of potatoes and other crops, even though the analytical sensitivity is low compared with column-equipped analytic instruments. Furthermore, FT-IR- and ^{1}H NMR-spectra-based multivariate analysis could be used to complement other analytical tools in the determination of substantial equivalence of genetically modified crops.

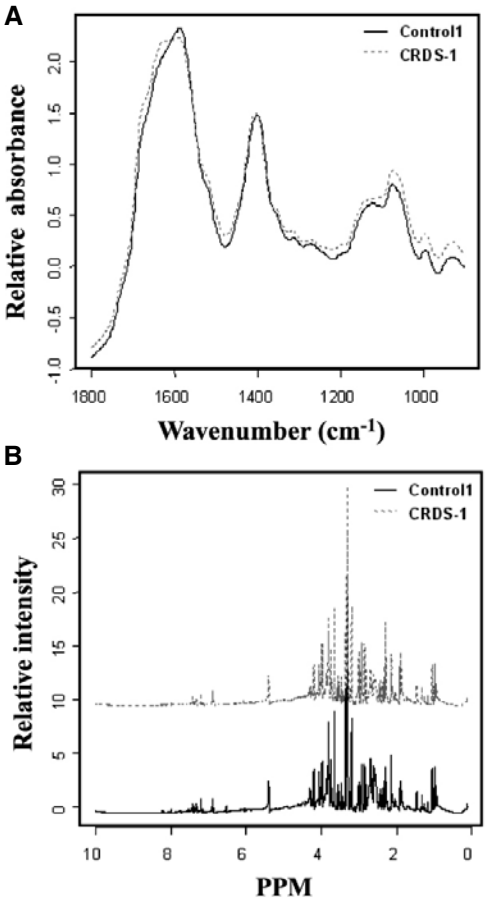

Fig. 10. Representative (A) FT-IR and (B) ^{1}H NMR spectra from wild-type (Control 1) and *CRDS*-expressing (*CRDS*-1) Desiree tubers.

CONCLUSION

Application of genetic engineering technology to crop plants has resulted in the production of many transgenic plants during the past decade. Because molecular engineering is widely used for major crop plants, methods for evaluation of changes in the metabolic profile are required and the effects of changes in the metabolite fingerprint on food safety must be considered. In particular, the safety of plant-derived vaccines has implications for human health. Based on the results obtained by the present study, we concluded that expression of human beta-amyloid, *CRDS* or *glgA* did not cause significant metabolic changes compared with the metabolic profile of wild-type potato tubers. Moreover, the method used in this study successfully detected differences in metabolic patterns between transgenic and non-transformed control plants, although we could not fully assign pure compounds. Because of the small number of transgenics examined in the present study, we cannot generalize the results to all transgenic potatoes, *i.e.* we cannot conclude that all transgenics are substantially equivalent to wild-type potatoes. However, in our study, results of the FT-IR and ^{1}H NMR spectral analyses clearly demonstrate that the transgenic lines examined were substantially equivalent to wild-type potatoes. Thus, we propose the combination of FT-IR and ^{1}H NMR spectral data and multivariate analysis as an efficient and rapid analytical tool for metabolic discrimination between transgenic and control lines of potatoes and other crops. Furthermore, FT-IR- and ^{1}H NMR-spectra-based multivariate analysis could be used to complement other analytical tools in the determination of substantial equivalence of genetically modified crops.

Acknowledgement This work was supported by grants from KRIBB Research Initiative Program and Plant Diversity Research Center of the 21st Century Frontier Research Program funded by Ministry of Education, Science and Technology of the Korean government.

Received July 6, 2009; accepted September 28, 2009

REFERENCES

1. Kok, E. J. and H. A. Kuiper (2003) Comparative safety assessment for biotech crops. *Trends Biotechnol.* 21: 439-444.
2. Catchpole, G. S., M. Beckmann, D. P. Enot, M. Mondhe, B. Zywicki, J. Taylor, N. Hardy, A. R. Smith, R. D. King, D. B. Kell, O. Fiehn, and J. Draper (2005) Hierarchical metabolomics demonstrates substantial compositional similarity between genetically modified and conventional potato crops. *Proc. Nat. Acad. Sci. USA* 102: 14458-14462.
3. Fiehn, O. and W. Weckwerth (2003) Deciphering metabolic networks. *Eur. J. Biochem.* 270: 579-588.
4. Krishnan, P., N. J. Kruger, and R. G. Ratcliffe (2005) Metabolite fingerprinting and profiling in plants using NMR. *J. Exp. Bot.* 56: 255-265.
5. Fiehn, O., J. Kopka, P. Dörmann, T. Altmann, R. N. Trethewey, and L. Willmitzer (2000) Metabolite profiling for plant functional genomics. *Nat. Biotech.* 18: 1157-1161.
6. Kaplan. F., J. Kopka, D. W. Haskell, W. Zhao, C. Schiller, N. Gatzke, D. Y. Sung, and C. L. Guy (2004) Exploring the temperature-stress metabolome of *Arabidopsis*. *Plant Physiol.* 136: 4159-4168.
7. Rohde, A., K. Morreel, J. Ralph, G. Goeminne, V. Hostyn, R. De Rycke, S. Kushnir, J. Van Doorsselaere, J. P. Joseleau, M. Vuylsteke, G. Van Driessche, J. Van Beeumen, E. Messens, and W. Boerjan (2004) Molecular phenotyping of the *pal1* and *pal2* mutants of *Arabidopsis thaliana* reveals far-reaching consequences on phenylpropanoid, amino acid, and carbohydrate metabolism. *Plant Cell* 16: 2749-2771.
8. Aharoni, A., C. H. Ric de vos, H. A. Verhoeven, C. A. Maliepaard, G. Kruppa, R. Bino, and D. B. Goodenowe (2002) Nontargeted metabolome analysis by use of Fou-

rier transform ion cyclotron mass spectrometry. *Omics* 6: 217-234.
9. Roessner, U., C. Wagner, J. Kopka, R. N. Trethewey, and L. Willmitzer (2000) Simultaneous analysis of metabolites in potato tuber by gas chromatography-mass spectrometry. *Plant J.* 23: 131-142.
10. Roessner, U., A. Luedemann, D. Brust, O. Fiehn, T. Linke, L. Willmitzer, and A. R. Fernie (2001) Metabolic profiling allows comprehensive phenotyping of genetically or environmentally modified plant systems. *Plant Cell* 13: 11-29.
11. Broeckling, C. D., D. V. Huhman, M. A. Farag, J. T. Smith, G. D. May, P. Mendes, R. A. Dixon, and L. W. Sumner (2005) Metabolic profiling of *Medicago truncatula* cell cultures reveals the effects of biotic and abiotic elicitors on metabolism. *J. Exp. Bot.* 56: 323-336.
12. Jeong, M. L., H. Jiang, H. S. Chen, C. J. Tsai, and S. A. Harding (2004) Metabolic profiling of the sink-to-source transition in developing leaves of Quaking Aspen. *Plant Physiol.* 136: 3364-3375.
13. Roessner, U., B. Hegemann, A. Lytovchenko, F. Carrari, C. Bruedigam, D. Granot, and A. Fernie (2003) Metabolic profiling of transgenic tomato plants overexpressing hexokinase reveals that the influence of hexose phosphorylation diminishes during fruit development. *Plant physiol.* 133: 84-99.
14. Takahashi, H., M. Hayashi, F. Goto, S. Sato, T. Soga, T. Nishioka, N. Tomita, M. Kawai-Yamada, and H. Uchimiya (2006) Evaluation of metabolic alteration in transgenic rice overexpressing dihydroflavonol-4-reduc-tase. *Ann. Bot.* 98: 819-825.
15. Colquhoun, I. J., G. L. Gall, K. A. Elliott, F. A. Mellon, and A. J. Michael (2006) Shall I compare thee to a GM potato? *Trends Genetics* 22: 525-528.
16. Le Gall, G., I. J. Colquhoun, A. L. Davis, G. J. Collins, and M. E. Verhoeyen (2003) Metabolite profiling of tomato (*Lycopersicon esculentum*) using ^{1}H NMR spectroscopy as a tool to detect potential unintended effects following genetic modification. *J. Agric. Food Chem.* 51: 2447-2456.
17. Oberdoerfer, R. B., R. D. Shillito, M. De Beuckeleer, and D. H. Mitten (2005) Rice (*Oryza sativa* L.) containing the bar gene is compositionally equivalent to the non-transgenic counterpart. *J. Agric. Food. Chem.* 53: 1457-1465.
18. Baker, J. M., N. D. Hawkins, J. L. Ward, A. Lovegrove, J. A. Napier, P. R. Shewry, and M. H. Beale (2006) A metabolomic study of substantial equivalence of field-grown genetically modified wheat. *Plant Biotechnol. J.* 4: 381-392.
19. Shewry, P. R., M. Baudo, A. Lovegrove, S. Powers, J. A. Napier, J. L. Ward, J. M. Baker, and M. H. Beale (2007) Are GM and conventionally bred cereals really? *Trends Food Sci. Technol.* 18: 201-209.
20. Youm, J. W., H. Kim, J. H. L. Han, C. H. Jang, H. J. Ha, I. M. Jung, J. H. Jeon, C. Y. Choi, Y. H. Kim, H. S. Kim, and H. Joung (2006) Transgenic potato expressing Aβ reduce Aβ burden in Alzheimer's disease mouse model. *FEBS Letts.* 579: 6737-6744.
21. Kim, H. S., J. W. Euym, M. S. Kim, B. C. Lee, I. Mook-Jung, J. H. Jeon, and H. Joung (2003) Expression of human β-amyloid peptide in transgenic potato. *Plant Sci.* 165: 1445-1451.
22. Kim, H. N. (2006) *Manipulation of photosynthesis and starch metabolism of potato by a cyanobasterial glycogen synthase.* Master's Thesis. Chungnam National University, Korea.
23. Murashige, T. and F. Skoog (1962) A revised medium for rapid growth and bioassays with tobacco tissue culture. *Plant Physiol.* 15: 473-497.
24. Stiller, I., G. Dancs, H. Hesse, R. Hoefgen, and Z. Bánfalvi (2007) Improving the nutritive value of tubers: elevation of cysteine and glutathione contents in the potato cultivar White Lady by marker-free transformation. *J. Biotechnol.* 128: 335-343.
25. Kwak, C. W., D. H. Choung, S. R. Min, S. W. Kim, J. R. Liu, and H. Chung (2007) Fast determination of ripeness stage of strawberries using infrared spectroscopy combined with principal component analysis. *Analytical Sci.* 23: 895-899.
26. Wong, J. W. H., G. Cagney, and H. M. Cartwright (2005) SpecAlign - processing and alignment of mass spectra datasets. *Bioinformatics* 21: 2088-2090.
27. Cellini, F., A. Chesson, I. Colquhoun, A. Constable, H. V. Davies, K. H. Engel, A. M. R. Gatehouse, S. Karenlampi, E. J. Kok, J. J. Leguay, S. Lehesranta, H. P. J. M. Noteborn, J. Pedersen, and M. Smith (2004) Unintended effects and their detection in genetically modified crops. *Food Chem. Toxicol.* 42: 1089-1125.
28. Shepherd, L. V. T., J. W. McNicol, R. Razzo, M. A. Taylor, and H. V. Davies (2006) Assessing the potential for unintended effects in genetically modified potatoes perturbed in metabolic and developmental processes: targeted analysis of key nutrients and anti-nutrients. *Transgenic Res.* 15: 409-425.